Natural variability of phytoplanktonic absorption in oceanic waters: Influence of the size structure of algal populations

Annick Bricaud, Hervé Claustre, Joséphine Ras, and Kadija Oubelkheir[1]
Laboratoire d'Océanographie de Villefranche, CNRS and Université Pierre et Marie Curie, Villefranche-sur-Mer, France

Received 5 April 2004; revised 12 July 2004; accepted 20 July 2004; published 19 November 2004.

[1] The spectral absorption coefficients of phytoplankton in oceanic waters were previously shown to vary with chlorophyll *a* concentration according to nonlinear relationships with a great deal of noise. We analyzed this biological noise on a data set of 596 simultaneous absorption and high-pressure liquid chromatography (HPLC) pigment measurements acquired within the surface layer (first optical depth) from various regions of the world's oceans. We observed systematic deviations from the average relationships for some oceanic areas and also seasonally within given areas. Using the detailed HPLC measurements, the influences of pigment composition and package effect (the two main sources of variability in algal absorption for a given chlorophyll *a* concentration) were explicitly separated for each sample. It was found that while the pigment composition experiences large variations, even within a restricted chlorophyll range, it is often not (at least within the first optical depth) the dominant source of the biological noise. Instead, these deviations mostly result from variability in the pigment packaging effect (for a given chlorophyll *a* concentration) due to variations in algal community size structure. This conclusion is fully confirmed by an independent approach, which consists of estimating a "size index" of algal populations from the relative concentrations of taxonomic pigments. *INDEX TERMS:* 4552 Oceanography: Physical: Ocean optics; 4847 Oceanography: Biological and Chemical: Optics; 4855 Oceanography: Biological and Chemical: Plankton; *KEYWORDS:* absorption, phytoplankton, optics

Citation: Bricaud, A., H. Claustre, J. Ras, and K. Oubelkheir (2004), Natural variability of phytoplanktonic absorption in oceanic waters: Influence of the size structure of algal populations, *J. Geophys. Res.*, *109*, C11010, doi:10.1029/2004JC002419.

1. Introduction

[2] The knowledge of light absorption coefficients of phytoplankton and their variations is central to the understanding of the optical variability of oceanic waters, and therefore to the refinement of "analytical" bio-optical models, in particular for ocean color interpretation. This knowledge is also needed to predict that part of light energy which is absorbed by algal cells and usable for photosynthesis. For these reasons, spectral absorption coefficients of algal populations ($a_\phi(\lambda)$), and their variations at different spatial and temporal scales, have been widely studied over the past years, in numerous regions of the world ocean [see, e.g., *Lohrenz et al.*, 2003; *Babin et al.*, 2003, and references therein]. These studies have shown that chl *a*-specific (i.e., per unit of chlorophyll *a* concentration) absorption coefficients, $a_\phi^*(\lambda)$, are variable due to changes in (1) cellular pigment composition and (2) pigment packaging effect. This effect, as predicted by theory, depends on cell size and intracellular pigment concentrations [*Kirk*, 1975; *Morel and Bricaud*, 1981]. Note that the variations in pigment composition or pigment packaging, resulting from population changes or from photoacclimation within a given population, generally reflect changes in environmental factors (available irradiance, nutrient concentration, etc.).

[3] In spite of their high variability, the $a_\phi^*(\lambda)$ coefficients were generally found to vary inversely to chl *a* concentration, and various parameterizations were proposed, either for selected wavelengths [e.g., *Prieur and Sathyendranath*, 1981; *Carder et al.*, 1991; *Cleveland*, 1995; *Ciotti et al.*, 1999; *Sathyendranath et al.*, 2001] or for the whole visible spectrum [*Bricaud et al.*, 1995, 1998; *Lee et al.*, 1998]. The statistical relationships observed between $a_\phi^*(\lambda)$ and chl *a* concentration indicate the existence of covariations between the chl *a* content, the proportions of accessory pigments relative to chl *a*, and the average size of algal populations. It is generally admitted that the average cell size increases from oligotrophic to eutrophic waters [e.g., *Malone*, 1980; *Yentsch and Phinney*, 1989; *Chisholm*, 1992], while the nonphotosynthetic pigments-to-chl *a* ratio tends to decrease [*Bricaud et al.*, 1995].

[4] In our previous studies [*Bricaud et al.*, 1995, 1998], while the existence of "average" a_ϕ versus chl *a* relationships was clearly demonstrated, we observed a large natural variability in $a_\phi(\lambda)$ around these relationships (e.g., a factor of 4 for a_ϕ (440), for a given chl *a* concentration). Such

[1]Now at Environmental Remote Sensing Group, CSIRO Land and Water, Canberra, ACT, Australia.

0148-0227/04/2004JC002419$09.00

Table 1. Information Concerning the Cruises Where Absorption and HPLC Data Were Simultaneously Collected[a]

Cruise	Location	Period	N	[Tchl *a*] Range, mg m^{-3}	TS
TOMOFRONT	northwestern Mediterranean	April 1990	9	0.155–0.957	M
EUMELI 3	tropical North Atlantic	Oct. 1991	5	0.073–0.340	O, M
FLUPAC	equatorial and subequatorial Pacific	Sep.–Oct. 1994	11	0.039–0.236	O
OLIPAC	equatorial and subequatorial Pacific	Nov. 1994	35	0.072–0.291	O
MINOS	eastern and western Mediterranean	May 1996	26	0.028–0.070	O
ALMOFRONT 2	Alboran Sea	Dec. 1997 and Jan. 1998	59	0.202–1.185	M
PROSOPE (upw)	Morocco upwelling	Sep. 1999	10	2.03–4.12	E
PROSOPE (Med)	eastern and western Mediterranean	Sep.–Oct. 1999	102	0.020–0.221	O
POMME 1	North Atlantic	Feb.–March 2001	87	0.105–0.928	M
POMME 2	North Atlantic	March–May 2001	83	0.254–1.44	M
POMME 3	North Atlantic	Aug.–Oct. 2001	108	0.039–0.312	O
BENCAL	Benguela upwelling	Oct. 2002	61	0.243–28.86	M, E

[a]The number of samples collected within the first optical depth (the only ones considered in this study) and the corresponding Tchl *a* (chl *a* + divinyl chl *a* + chlorophyllid *a* + pheopigments) range are indicated for each cruise. The dominant trophic state (TS) is indicated (E, eutrophic; M, mesotrophic; O, oligotrophic).

natural variability could explain why the a_ϕ versus chl *a* concentration relationships have been found in some occasions to differ between regions [e.g., *Carder et al.*, 1991; *Cleveland*, 1995; *Lutz et al.*, 1996; *Bricaud et al.*, 2000; *Sathyendranath et al.*, 2001]. In our data set, this natural variability was difficult to analyze, because measurements by high-pressure liquid chromatography (HPLC) were not available for all cruises, and the detailed pigment composition was known only for a few regions. Since then, our absorption spectra data set has been increased with data from recent cruises (either in geographic regions not explored previously, or in regions previously sampled but in different seasons), and HPLC measurements were systematically acquired.

[5] The aim of the present paper is to use this increased data set to examine the causes of the variability in $a_\phi(\lambda)$, by separating explicitly the impact of pigment composition changes and that of pigment packaging changes, which in the surface layer are mostly related to cell size. Such an explicit separation was attempted in several studies, using various methods [*Nelson et al.*, 1993; *Lutz et al.*, 1996; *Stuart et al.*, 1998; *Ciotti et al.*, 2002; *Lohrenz et al.*, 2003]. In these studies, the information concerning the size structure of populations was provided (generally for selected samples) by flow cytometric or microscopic analyses, or measurements on size-fractionated samples. These methods, however, are often difficult to operate routinely for systematic measurements. The size distribution of particles can also be measured at sea with a particle counter, but then it is difficult to extract the information concerning the size distribution of algal cells only, which is generally obscured by that of accompanying nonalgal particles. Recently, it has been proposed [*Vidussi et al.*, 2001; J. Uitz et al., From surface chlorophyll *a* to phytoplankton community composition in oceanic waters, submitted to *Global Biogeochemical Cycles*, 2004, hereinafter referred to as Uitz et al., submitted manuscript, 2004] to use the HPLC information to derive indices related to the size structure of algal populations. These indices, based on the relative concentrations of some taxonomic (or "diagnostic") pigments, are proxies of the relative biomass proportions of picophytoplankton, nanophytoplankton, and microphytoplankton. This new method provides the opportunity of estimating the dominant size within algal populations, and thus the role of cell size changes in the observed variability of a_ϕ.

2. Materials and Methods

2.1. Sampling

[6] Samples were collected during eleven cruises, in different seasons and around the world's oceans between 1990 and 2002 (Table 1). All the data here considered exclusively correspond to oceanic-case 1 waters. The data from the five first cruises listed in Table 1 were already described and used in the work of *Bricaud et al.* [1998]; data from other cruises in this previous paper are no longer considered here, as no HPLC measurements were performed. The present data set includes additional data, collected during six cruises performed between 1997 and 2002 (see Table 1). Only samples collected within the first optical depth are considered in this study, so as to minimize the influence of photoacclimation, which may modify the packaging effect, and consequently absorption coefficients, in a similar way to cell size [e.g., *Morel and Bricaud*, 1981]. The first optical depth was computed for each station as being $z_{eu}/4.6$, where z_{eu}, the euphotic depth, is the depth where the photosynthetically available radiation is reduced to 1% of its value just below the surface. The euphotic depth was either determined in the field, or computed from the chlorophyll profile according to *Morel and Maritorena* [2001]. From a total of 4105 samples, 596 belong to the first optical depth and are considered in the present study.

2.2. Pigment and Spectral Absorption Measurements

[7] Methods employed for particulate and algal absorption measurements are described in detail in the work of *Bricaud et al.* [1998]. In summary, particulate absorption coefficients were measured using the "quantitative glass-fiber filter technique" (QFT), except for the FLUPAC cruise where the "glass-slide technique" [*Allali et al.*, 1995] was used. With this latter technique, absorption measurements are not affected by the path length amplification effect ("β effect"). When the QFT was used, all spectra were corrected for the β effect, using the algorithms given by *Allali et al.* [1997] for samples collected in oligotrophic sites (OLIPAC, MINOS, the Mediterranean part of PROSOPE, and POMME 3 cruises; see Table 1), and by *Bricaud and*

Stramski [1990] for all other samples. The need for a modified algorithm for picophytoplankton-dominated waters has been demonstrated in an earlier study [*Allali et al.*, 1997]. The values provided by the two algorithms differ by 30 to 35% at the most, according to the optical density. Finally, the respective contributions of phytoplankton and nonalgal particulate matter to total particulate absorption were determined by numerical decomposition [*Bricaud and Stramski*, 1990], except for the TOMOFRONT and EUMELI 3 cruises where they were determined experimentally [*Kishino et al.*, 1985]. For most cruises where the numerical decomposition method was applied, experimental determinations were performed on selected samples to locally check the validity of the used assumptions.

[8] Pigment concentrations were measured by high-pressure liquid chromatography (HPLC), using the procedure described by *Claustre and Marty* [1995] for the TOMOFRONT and EUMELI 3 cruises, and by *Vidussi et al.* [1996] for all other cruises. With the latter method, chl *a* and divinyl-chl *a* are fully resolved. Up to twenty pigments were identified for each sample. The concentrations of pheopigments (pheophytin and pheophorbide) were generally negligible, except in eutrophic waters (Morocco and Benguela upwelling areas). In what follows, the pheopigment concentration is added to the chlorophyll *a*, divinyl-chl *a* and chlorophyllid *a* concentrations, the sum is referred to as "Tchl *a* concentration," and noted [Tchl *a*]. Absorption coefficients of phytoplankton were converted into chl-specific absorption coefficients (a_ϕ*) by normalizing to [Tchl *a*].

2.3. Size Structure of Algal Populations

[9] The relative biomass proportions of picophytoplankton (<2 μm), nanophytoplankton (2–20 μm) and microphytoplankton (20–200 μm) in natural populations were estimated from the concentrations of those pigments which have a taxonomic significance and can be associated to a size class, at least in oceanic case 1 waters [*Vidussi et al.*, 2001]. The biomass proportions associated with each size class were computed as

$$\%\ \text{picophytoplankton} = 100 * (0.86[\text{zeaxanthin}] + 1.01[\text{chl } b + \text{divinyl-chl } b])/\text{DP} \quad (1a)$$

$$\%\ \text{nanophytoplankton} = 100 * (0.60[\text{alloxanthin}] + 0.35[19'\text{-BF}] + 1.27[19'\text{-HF}])/\text{DP} \quad (1b)$$

$$\%\ \text{microphytoplankton} = 100 * (1.41[\text{fucoxanthin}] + 1.41[\text{peridinin}])/\text{DP}, \quad (1c)$$

where DP is the sum of the weighted concentrations of all diagnostic pigments:

$$\text{DP} = (0.86[\text{zeaxanthin}] + 1.01[\text{chl } b + \text{divinyl-chl } b] + 0.60[\text{alloxanthin}] + 0.35[19'\text{-BF}] + 1.27[19'\text{-HF}] + 1.41[\text{fucoxanthin}] + 1.41[\text{peridinin}]). \quad (1d)$$

The numerical coefficients in these relationships were computed by multiple regression and represent the average ratio of Tchl *a* to each accessory pigment (Uitz et al., submitted manuscript, 2004). Although this method provides only approximate proportions (in some occasions, a given diagnostic pigment is shared by two size classes), it provides reliable results at regional [*Vidussi et al.*, 2001] as well at global scale (Uitz et al., submitted manuscript, 2004).

[10] In order to synthesize the above information, a "size index" was derived from these proportions, by attributing a central size value to each size class (1 μm, 5 μm and 50 μm for picophytoplankton, nanophytoplankton, and microphytoplankton, respectively) and weighing this value by the biomass proportion of the corresponding class, i.e.,

$$\text{SI}(\mu\text{m}) = [1 * (\%\ \text{picoplankton}) + 5 * (\%\ \text{nanoplankton}) + 50 * (\%\ \text{microplankton})]/100. \quad (2)$$

This size index is obviously only a very rough indicator of the dominant size of the algal population, because each size class is represented by a unique (central) size. In spite of its approximate character, this index presents the advantage to vary continuously (from 1 μm for pure picophytoplankton, likely prokaryotes, to 50 μm for pure microphytoplankton, likely diatoms), and thus provides a single parameter, characterizing the size structure of algal populations.

2.4. Computation of the Package Effect Index

[11] For a given algal population, the "package effect index," $Q_a^*(\lambda)$, is defined as the ratio of the actual absorption coefficient, $a_\phi(\lambda)$, to the absorption coefficient of the same material which would be dispersed into solution, $a_{sol}(\lambda)$ [*Morel and Bricaud*, 1981]:

$$Q_a^*(\lambda) = a_\phi(\lambda)/a_{sol}(\lambda). \quad (3)$$

This index decreases from 1 (no package effect) to 0 (maximal package effect). The absorption coefficients $a_{sol}(\lambda)$ (in m^{-1}) can be obtained by summing the contributions of all individual pigments, using the relationship:

$$a_{sol}(\lambda) = \Sigma\ C_i\ a^*_{sol,i}(\lambda), \quad (4)$$

where the $a^*_{sol,i}$ coefficients are the weight-specific absorption spectra of individual pigments (in $m^2\ mg^{-1}$), and C_i are their concentrations in the medium (in mg m^{-3}). The $a^*_{sol,i}$ spectra were estimated by scaling the absorption spectra of individual pigments in solvent, measured in relative values by HPLC, to the weight-specific absorption coefficients proposed by *Goericke and Repeta* [1993], and then shifting the positions of maxima to their in vivo positions, as in the work of *Bidigare et al.* [1990] (Figure 1).

[12] When applying equations (3) and (4), we observed that Qa* was higher than 1 (i.e., measured absorption values were higher than those reconstructed using equation (4)) for many samples, and particularly for those collected in oligotrophic waters. As similar observations were made by several authors (see references in Appendix A), we hypothesized that a term is missing when

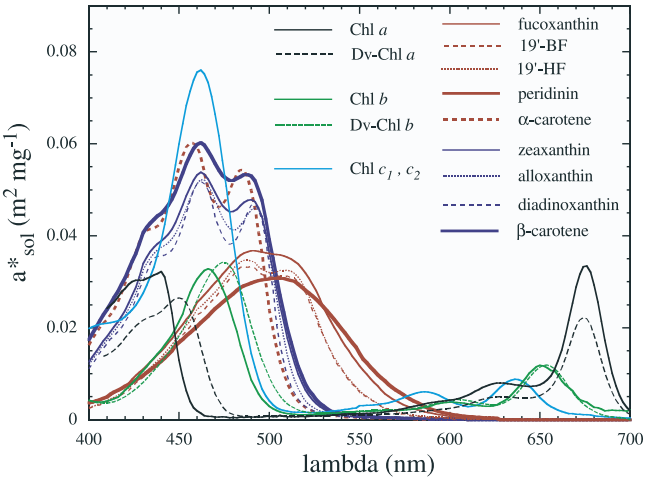

Figure 1. Assumed in vivo weight-specific absorption spectra of the main pigments, $a^*_{sol,i}(\lambda)$ (in m^2 mg^{-1}), as derived from absorption spectra of individual pigments in solvent (see text). Absorption spectra of photosynthetic and nonphotosynthetic carotenoids are shown in red and blue, respectively.

reconstructing the in vivo absorption spectrum of natural populations from pigment concentrations. The existence and formulation of this "missing term" are discussed in more detail in Appendix A. Equation (4) was thus modified as follows:

$$a_{sol}(\lambda) = a_{pigm}(\lambda) + a_{miss}(\lambda), \qquad (4')$$

with

$$a_{pigm}(\lambda) = \Sigma\, C_i\, a^*_{sol,i}(\lambda) \qquad (4'')$$

and

$$a_{miss}(440) = 0.0525[\text{Tchl } a]^{0.855}, \qquad (4''')$$

(see Appendix A). The package effect index at 440 nm, Qa*(440), was therefore derived from equations (3) and (4′). Because this correction is empirical and was derived from measurements on a limited number of samples, it is acknowledged that the absolute values of Q_a^* have to be considered with precaution. The relative variations of Q_a^* which will be discussed hereafter, however, are only weakly affected by the above correction.

3. Results and Discussion

3.1. Phytoplanktonic Absorption as Related to Chlorophyll *a* Concentration: Average Relationships and Deviations

[13] The variations of the a_ϕ coefficient at 440 nm, as a function of [Tchl *a*], are shown in Figure 2a. As previously observed [*Bricaud et al.*, 1995, 1998], $a_\phi(440)$ increases with [Tchl *a*] according to a power function, and a least square fit provides the following relationship:

$$a_\phi(440) = 0.0654[\text{Tchl } a]^{0.728} \qquad (r^2 = 0.934,\ N = 596). \quad (5)$$

This relationship can be compared to that obtained when the *Bricaud et al.* [1995] data set is restricted to samples collected within the first optical depth:

$$a_\phi(440) = 0.0383[\text{Tchl } a]^{0.651}. \qquad (5')$$

It appears that the a_ϕ (440) values for the present data set are shifted toward higher values, by approximately 60% (note that the data sets in these two studies are almost independent, as only 14 samples, from the TOMOFRONT and EUMELI 3 cruises, are common to both). This shift is partly, but not exclusively, due to the fact that in the present data set, [Tchl *a*] was measured only by HPLC. Actually, equations (5) and (5′) are representative of two groups of cruises: (1) one group which includes FLUPAC, OLIPAC, POMME 1, POMME 2, and BENCAL cruises, and is well represented by equation (5), (2) another group, including mainly MINOS and ALMOFRONT 2 samples, and is closer to equation (5′). The values corresponding to the PROSOPE and POMME 3 cruises fall mostly between the two regression lines and represent intermediate situations (while those for TOMOFRONT and EUMELI 3 cruises are scattered). Note that these features, which are still observed for the wavelength 490 nm (Figure 2b), practically disappear at 676 nm (Figure 2c).

[14] Therefore some deviations from the global "average relationship" (represented by equation (5)) appear, which can be examined by considering specific [Tchl *a*] ranges. For sake of simplification, we will call hereafter "oligotrophic" those waters with [Tchl *a*] < 0.2 mg m^{-3}, "mesotrophic" those with [Tchl *a*] between 0.2 and 2 mg m^{-3}, and "eutrophic" those with [Tchl *a*] > 2 mg m^{-3}. In the domain of "eutrophic" waters, the a_ϕ(440) values for the PROSOPE cruise (Morocco upwelling site) are lower, by 20–30%, than

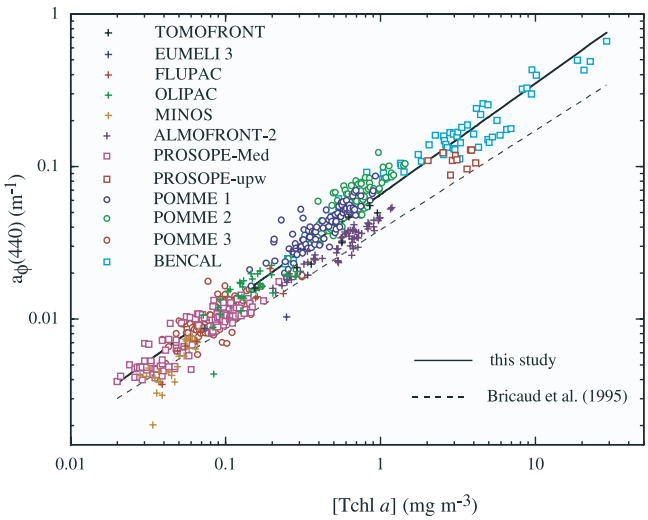

Figure 2a. Variations of the absorption coefficients of phytoplankton at 440 nm as a function of the Tchl *a* concentration, for the various cruises (see Table 1). Only samples collected within the first optical depth have been considered in these figures and all following ones. The regression line (equation (5)) is shown as a solid line. The relationship obtained by *Bricaud et al.* [1995] (equation (5′)) is shown for comparison as a dashed line.

those corresponding to the BENCAL cruise (Benguela upwelling). For "mesotrophic" waters, the $a_\phi(440)$ values for the ALMOFRONT-2 cruise are also lower, by approximately 30%, than those corresponding to the POMME 1 and POMME 2 cruises. In the domain of "oligotrophic" waters, the differences are less marked, however the lowest $a_\phi(440)$ values are observed for the MINOS cruise. Note that the MINOS and PROSOPE cruises have taken place in the same geographical location (western Mediterranean and Ionian Sea), but in different seasons (spring and late summer, respectively; see Table 1).

[15] In order to analyze quantitatively these deviations, it is necessary to take into account the possible sources of variation, and to determine their relative contributions. It is recalled that for a given Tchl *a* content, variations in $a_\phi(\lambda)$ can be induced by (1) variations in the proportions in accessory pigments relatively to [Tchl *a*], (2) variations in the package effect, which, in turn, are governed by variations in the size structure of populations, and/or in the intracellular concentrations of the various pigments.

[16] As the influences of pigment composition and of package effect upon absorption are both maximal around 440 nm, we select this wavelength to examine their compared variations. By combining equations (3) and (4′), it comes:

$$a_\phi(440) = \left[a_{pigm}(440) + a_{miss}(440)\right] \times Q_a^*(440), \qquad (6)$$

where the two main factors of variability, $a_{pigm}(440)$ and $Q_a^*(440)$, appear explicitly (a third factor of variability, the biological noise likely affecting the $a_{miss}(440)$ versus [Tchl *a*] relationship (equation (4‴)) has been neglected here). In what follows, we will examine successively the actual variations in pigment composition and in size structure within our data set. Then the respective impacts of these two sources of variability upon $a_\phi(440)$ will be compared, via the terms $a_{pigm}(440)$ and $Q_a^*(440)$.

3.2. Variations in the Pigment Composition of Algal Populations

[17] In view of examining the variability in pigment composition within our data set, we have grouped the accessory pigments into four main categories, according to their similarities in spectral absorption characteristics (see Figure 1): (1) chl *b* and divinyl chl *b* (noted Tchl *b*); (2) chl c_1, c_2 and c_3 (noted Tchl *c*); (3) photosynthetic carotenoids (noted PSC), i.e., fucoxanthin, peridinin, 19′-HF and 19′-BF; (4) nonphotosynthetic carotenoids (noted PPC), i.e., zeaxanthin, diadinoxanthin, alloxanthin, and β-carotene. We have also included in this latter category two photosynthetic carotenoids, lutein and α-carotene, because their absorption spectra are similar to those of zeaxanthin and β-carotene, respectively (in addition, for several cruises, only the sums of (zeaxanthin + lutein) and (α + β carotene concentrations were measured by HPLC). These two pigments, always in low concentration in the surface layer, affect the PPC concentration only weakly.

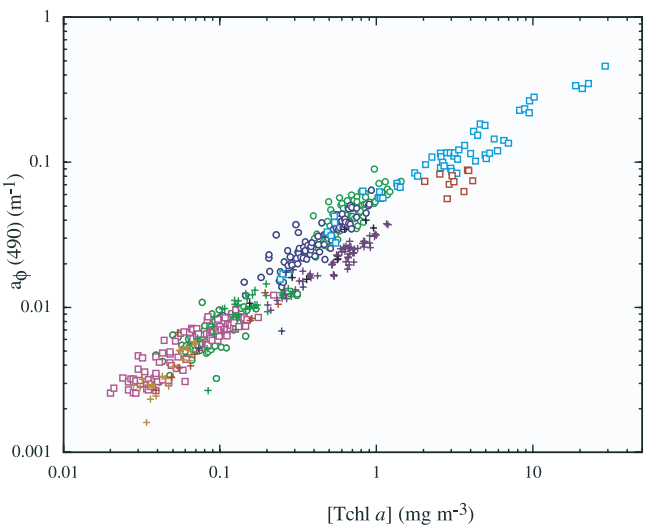

Figure 2b. As Figure 2a, for the wavelength 490 nm.

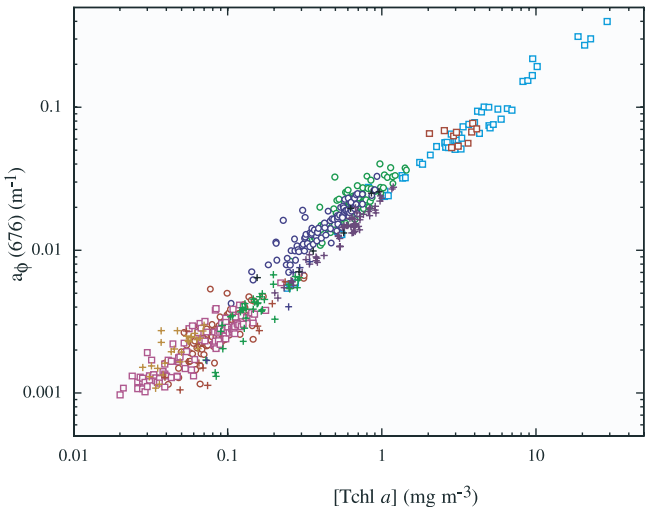

Figure 2c. As Figure 2a, for the wavelength 676 nm.

[18] The proportions of the four categories of accessory pigments, relatively to the Tchl *a* concentration, are highly variable from one cruise to the other, and also within cruises (Figure 3). The [Tchl *b*]/[Tchl *a*] ratio varies for most samples between 0 and 0.2, except for the POMME 1 cruise where it can reach values as high as 0.6. The [Tchl *c*]/[Tchl *a*] ratio shows a trend to increase with the Tchl *a* concentration, from less than 0.1 in the clearest waters ([Tchl *a*] < 0.1 mg m^{-3}) to about 0.2 for [Tchl *a*] = 1 mg m^{-3}. Two clusters of points deviate from this general trend: the POMME 2 samples, for which the ratio may be as high as 0.4, and those corresponding to eutrophic waters (Morocco and Benguela upwelling areas), for which the ratio remains most often below 0.2.

[19] The proportions of carotenoids, relatively to [Tchl *a*], are even more variable. The [PSC]/[Tchl *a*] ratio varies for most samples between 0 and 1 (with the exception of a few TOMOFRONT samples where values up to 2 are found), with no particular trend with respect to the Tchl *a* concentration. The [PPC]/[Tchl *a*] ratio (mostly determined by the (zeaxanthin)/[Tchl *a*] ratio) reveals a distinct trend to decrease with [Tchl *a*], with the lowest values (around 0.1) in mesotrophic waters (POMME 2 cruise) and in the Morocco upwelling area, and the highest values (up to 1.4) in the oligotrophic waters of the equatorial Pacific (FLUPAC and OLIPAC samples). Note that with similar [Tchl *a*] ranges, oligotrophic Mediterranean waters (MINOS,

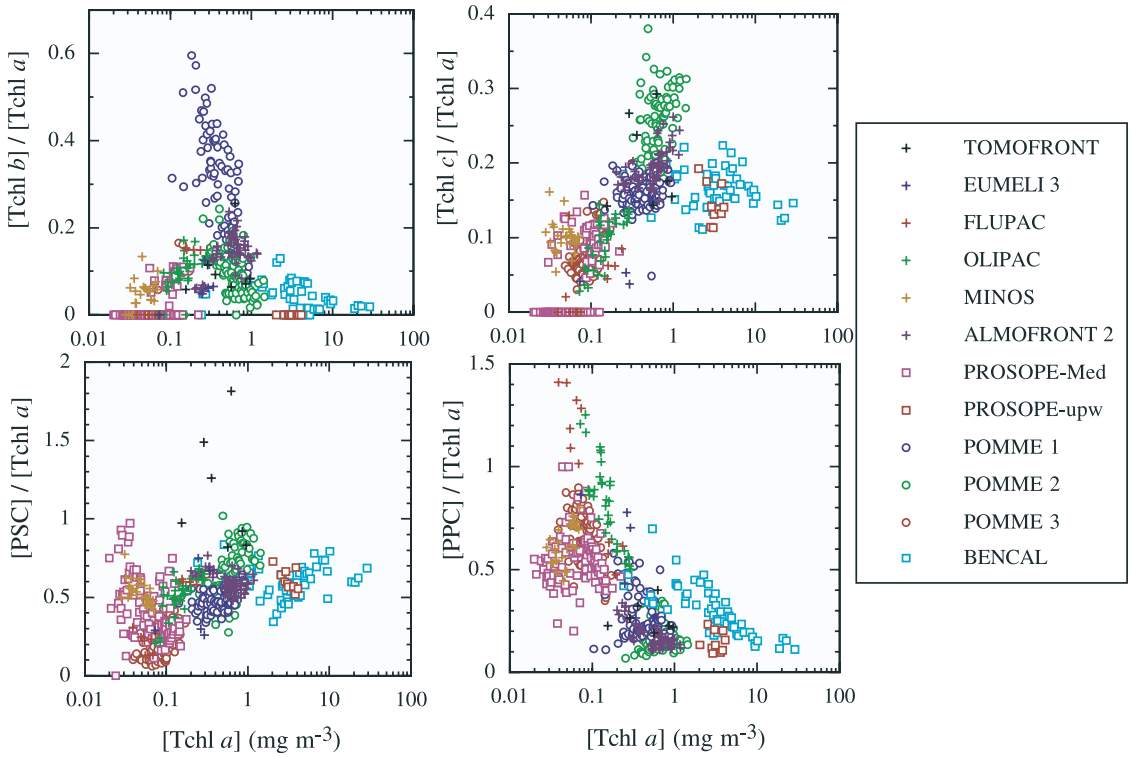

Figure 3. Variations of the accessory pigments to Tchl *a* ratios as a function of Tchl *a* concentration.

PROSOPE) reveal much lower values for this ratio (mostly from 0.3 to 0.8).

[20] In summary, a very large diversity in pigment composition is observed within our data set. Because the various pigments can compensate their effects, however, this is not necessarily reflected in absorption coefficients, and the actual impact of pigment composition will have to be examined, through the term $a_{pigm}(440)$ (see later).

3.3. Variations in the Size Structure of Algal Populations

[21] The respective contributions of picophytoplankton, nanophytoplankton, and microphytoplankton to total algal biomass for each sample, as derived from equations (1a)–(1c), are displayed using a ternary plot (Figure 4). It can be observed that the size structure of algal populations is highly variable from one oceanic area to the other, and also within a given area. However, some clusters of points are observed, generally in relation to the [Tchl *a*] range covered for each cruise (see Table 1).

[22] Eutrophic waters from the Morocco and Benguela upwelling areas (PROSOPE and BENCAL cruises) are mostly dominated by microphytoplankton. Samples from the Morocco upwelling contain a small proportion of nanophytoplankton (10 to 20%) and no picophytoplankton. A few samples from the Benguela upwelling area, close to the apex, contain 85–95% of microphytoplankton, while waters off the upwelling area reveal more mixed populations, where microphytoplankton is progressively replaced by nanophytoplankton (which increases up to 70%) and picophytoplankton (which increases up to 45%).

[23] Mesotrophic waters from the Mediterranean frontal areas (TOMOFRONT and ALMOFRONT 2 cruises) reveal a low amount of picophytoplankton (10 to 30% of total biomass), and are dominated by both nanophytoplankton and microphytoplankton (30–80% for nanophytoplankton, 10–50% for microphytoplankton). Mesotrophic waters from the North Atlantic (POMME 1 and 2), while having a [Tchl *a*] range similar to that of Mediterranean frontal areas (see Table 1), reveal a different size structure. For the POMME 1 cruise, the size structure is closer to that of oligotrophic waters (microphytoplankton <15% of total biomass), with populations dominated by both nanophytoplankton and picophytoplankton. Waters from the POMME 2 cruise are largely dominated by nanophytoplankton (>70% for most samples).

[24] Most oligotrophic waters from the Mediterranean (PROSOPE cruise), the equatorial Pacific (FLUPAC, OLIPAC), and the North Atlantic (POMME 3) are characterized by a very low (0 to 10%) contribution of microphytoplankton, and variable contributions both for picophytoplankton and nanophytoplankton. For numerous samples from the PROSOPE and POMME 3 cruises, microphytoplanktonic populations are totally absent, and the highest proportions of picophytoplankton (60 to 90%) are observed for POMME 3. Note also that many samples from the MINOS cruise depart from the group of oligotrophic waters, as they contain a higher proportion of microphytoplankton (15 to 20% of algal biomass) and less picophytoplankton (<40%).

[25] These observations can be summarized by considering the variations of size index (computed using equation (2)) as a function of [Tchl *a*] (Figure 5). While a general covariation between [Tchl *a*] and size index is observed, some deviations appear. For instance, the size indices for the Morocco upwelling (PROSOPE cruise) are close to the maximum value (50 μm, 100% microphytoplankton) while those in the same [Tchl *a*] range for the Benguela upwelling (BENCAL cruise) are generally lower

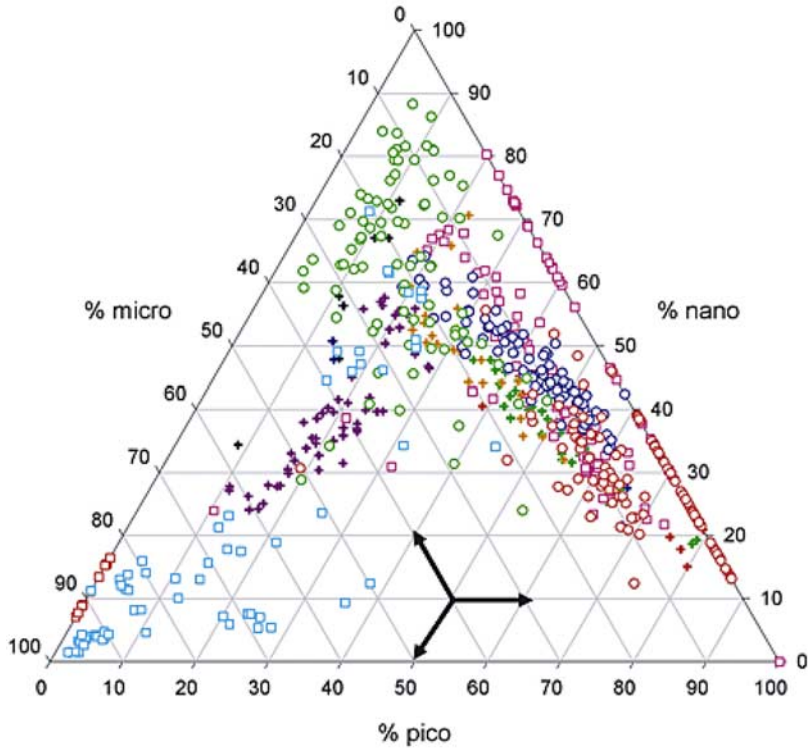

Figure 4. Ternary plot showing the relative contributions (percent) of picophytoplankton, nanophytoplankton, and microphytoplankton to total biomass, estimated from the relative concentrations of some taxonomic pigments (equations (1a)–(1c)). The symbols are as in Figure 3. For each sample the relative contribution of a size class to total biomass can be read on the corresponding axis as indicated.

(25–40 μm). In the same way, the size indices for TOMOFRONT and ALMOFRONT 2 samples (between 15 and 40 μm) are on average larger than those corresponding to other mesotrophic waters (POMME 1 and 2, between 5 and 20 μm). The size indices for waters from the MINOS cruise (around 10–15 μm) are larger (for equivalent Tchl *a* contents) than those observed for other oligotrophic waters. Therefore, even if a general covariation between size structure (or size index) and [Tchl *a*] is actually observed, the above observations suggest that even in surface waters, the size structure of algal populations may vary significantly for a given Tchl *a* content.

3.4. Compared Impacts of Pigment Composition and Package Effect Upon Absorption Coefficients

[26] Knowing the weight-specific absorption coefficients of all individual pigments (see Figure 1) and their concentrations for each sample, equation (4″) can be used to estimate the absorption coefficient of the pigment pool at 440 nm, $a_{pigm}(440)$, for a given sample. After normalization by [Tchl *a*], the chl *a*-specific coefficients, $a^*_{pigm}(440)$, are obtained (Figure 6). As stated before, this term allows the actual impact of pigment composition variations upon $a_\phi(440)$ to be quantified.

[27] Then, using equation (6), the variations of $Q_a^*(440)$ versus [Tchl *a*] can be assessed for the various cruises (Figure 7). The compared variations of size index (Figure 5), $Q_a^*(440)$ (Figure 7) and $a^*_{pigm}(440)$ (Figure 6) enable us to appreciate, for a given [Tchl *a*] range, the dominant cause of variability in $a_\phi(440)$. It must be emphasized here that the variations of size index and of $Q_a^*(440)$ are obtained using totally independent approaches (equations (2) and (6)).

[28] It must be recalled also that the size index is directly derived from the concentrations of some taxonomic pigments, which clearly indicates that changes in cell size and in pigment composition are highly correlated in the field (as both resulting mostly from population changes). This correlation, however, does not hinder a separate evaluation of

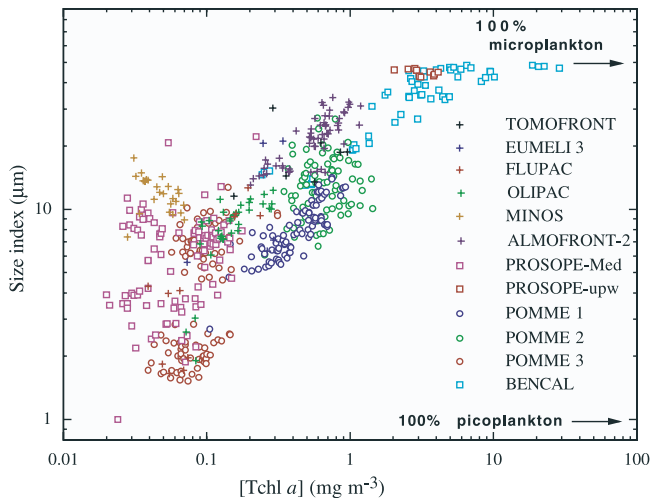

Figure 5. Variations of the size index, estimated using equation (2), as a function of the Tchl *a* concentration.

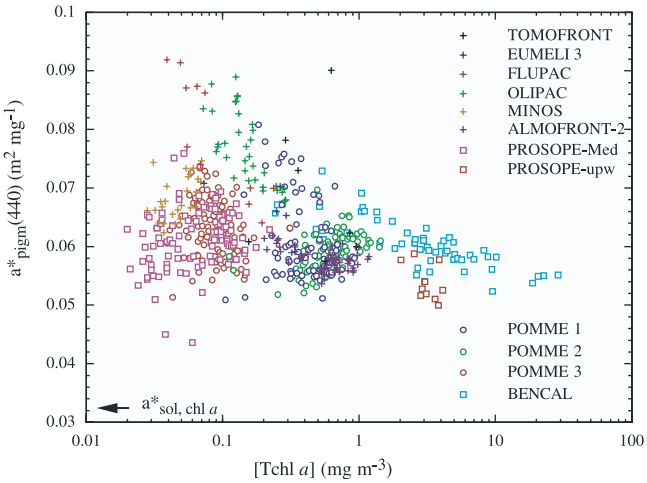

Figure 6. Variations of the chl-specific absorption coefficient of pigments at 440 nm, $a^*_{pigm}(440)$ (obtained by using equation (4″) and then normalizing by the Tchl *a* concentration), as a function of the Tchl *a* concentration.

the direct effects of pigment composition (through $a^*_{pigm}(440)$) and cell size (through $Q_a^*(440)$) upon $a_\phi(440)$.

3.4.1. Eutrophic Waters

[29] In these waters, the $a_\phi(440)$ values have been previously observed to be (for equivalent Tchl *a* contents) lower by 20–30% in the Morocco upwelling (PROSOPE cruise) than in the Benguela upwelling (BENCAL cruise; Figure 2a). Consistently, the values of $a^*_{pigm}(440)$ are approximately 15% lower (Figure 6), mostly due to lower PPC/Tchl *a* ratios, and to the absence of chl *b* in the Morocco upwelling area (Figure 3). On the other hand, size index values for the Morocco upwelling area are on average larger, and consistently, Qa*(440) values are smaller than for the Benguela upwelling. Here the differences in pigment composition and size structure appear to combine their effects and both explain the differences in $a_\phi(440)$ between the two upwelling areas.

3.4.2. Mesotrophic Waters

[30] The $a_\phi(440)$ values for the Mediterranean (ALMOFRONT-2 and TOMOFRONT) cruises are lower, by approximately 30%, than for the Atlantic (POMME 1 and POMME 2) cruises (Figure 2a). Most of the values of $a^*_{pigm}(440)$ for these cruises, however, cover essentially the same range, 0.54–0.64 $m^2\ mg^{-1}$ (except for a few samples from POMME 1 with a high chl *b* content; Figure 6). In contrast, the size index values are significantly higher for the Mediterranean samples (about 15 to 40 μm) than for the Atlantic samples (about 5 to 20 μm; Figure 5), and in parallel, their Qa*(440) values are lower (0.2–0.4 instead of 0.3–0.7; Figure 7). This suggests that for these waters, the variability in $a_\phi(440)$ (for a given [Tchl *a*]) is primarily influenced by the variations in the size structure of algal populations, whereas the pigment composition has a reduced effect.

3.4.3. Oligotrophic Waters

[31] In this domain ([Tchl a] < 0.2 mg m^{-3}), samples from the MINOS cruise show the lowest $a_\phi(440)$ values (Figure 2a). The $a^*_{pigm}(440)$ values for these samples are in the same range as those from the PROSOPE and POMME 3 cruises (Figure 6). It is remarkable, however, that they show the highest size indices (10–15 μm, Figure 5). Consistently, they also reveal the lowest Qa*(440) values in the considered Tchl *a* domain (mostly in the range 0.4–0.7, while values for other cruises are closer to 1), indicating a stronger package effect (Figure 7). Therefore, as for mesotrophic waters, the size structure appears here to have a dominant influence upon the variations in a_ϕ (440).

[32] Note also that the highest $a^*_{pigm}(440)$ values are observed for the FLUPAC and OLIPAC cruises, characterized by very high PPC/Tchl *a* ratios (see Figure 3). This is, however, compensated by the rather high values of size index (around 7–10 μm) compared to other oligotrophic waters, so that these high $a^*_{pigm}(440)$ values do not have a strong impact on $a_\phi(440)$ (Figure 2a).

[33] When comparing Figures 5 and 7, it is striking to note that for a given [Tchl *a*] range, the groups of samples with a size index in the upper range generally exhibit $Q_a^*(440)$ values in the lower range. It is recalled that the package effect is determined not only by the size structure, but also by photoacclimation phenomena which modify the intracellular pigment concentrations. Even if the data set is restricted to the first optical depth, these photoacclimation phenomena are expected to be variable from one cruise to the other, and even within a given cruise, as a response to variable surface lighting conditions. The opposite variations of size index and Qa*(440) suggest that (1) size index and Qa*(440), obtained by using independent approaches, vary consistently, (2) for the present data set, the size structure is the predominant factor ruling $Q_a^*(440)$. To go beyond this qualitative observation, it is interesting to check if the values of $Q_a^*(440)$ and of size index are quantitatively consistent with each other, and agree with theoretical predictions.

3.5. Experimental Relationship Between Package Effect Index and Size Index

[34] For a monodispersed population, the theoretical variations of Q_a^* are related to those of the product (a_{cm}.d), d), where d is the cell size and a_{cm} is the absorption

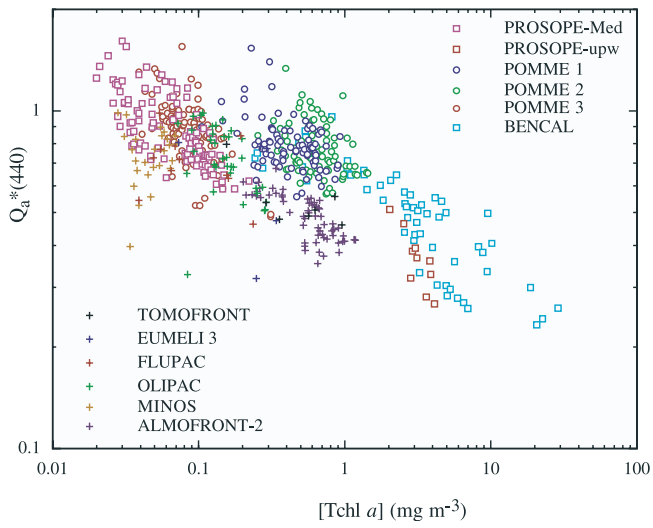

Figure 7. Variations of the package effect at 440 nm, $Q_a^*(440)$ (computed using equation (6)), as a function of the Tchl *a* concentration.

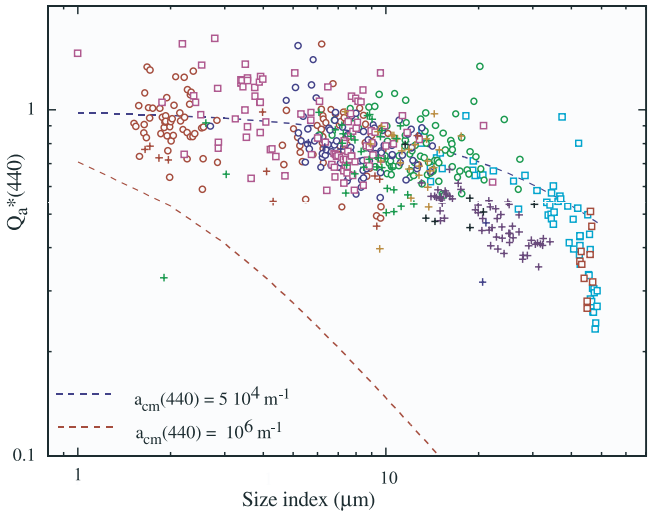

Figure 8. Variations of the package effect at 440 nm, $Q_a^*(440)$, as a function of the size index. The symbols are as in Figure 7. The dashed lines represent the theoretical $Q_a^*(440)$ versus cell size relationships, for two values of the absorption coefficient of cellular matter at 440 nm, $a_{cm}(440)$, delimiting a representative range for phytoplanktonic cells (see text).

coefficient of cellular matter, through the relationship [*Morel and Bricaud*, 1981]:

$$Q_a^*(a_{cm}.d) = (3/2)Q_a(a_{cm}.d)/(a_{cm}.d), \quad (7)$$

where Q_a represents the efficiency factor for absorption:

$$Q_a(a_{cm}.d) = 1 + 2^* \exp(-a_{cm}.d)/(a_{cm}.d) + 2^*[\exp(-a_{cm}.d) - 1]/(a_{cm}.d)^2, \quad (8)$$

[*Van de Hulst*, 1957]. The a_{cm} coefficient is also linked to the imaginary part of refractive index of cells, n', by the simple relationship:

$$a_{cm} = 4\ \pi\ n'/\lambda. \quad (9)$$

[35] Using equation (9), realistic values for $a_{cm}(440)$ can be derived from the study of *Stramski et al.* [2001], who have provided the values of $n'(440)$ for 23 phytoplanktonic species, ranging from picophytoplankton to large diatoms, and grown under various lighting conditions. The observed range of variation in n', $2.2\ 10^{-3}$ to $2.3\ 10^{-2}$, leads to $a_{cm}(440) = 8.4\ 10^4$ to $8.7\ 10^5\ m^{-1}$, with the highest values corresponding to picophytoplanktonic species or to low lighting conditions. We therefore selected $5\ 10^4$ to $10^6\ m^{-1}$ as a realistic range of variation for $a_{cm}(440)$. The theoretical $Q_a^*(440)$ versus cell size curves, for these two extreme values, can be compared to the experimental values of $Q_a^*(440)$, plotted as a function of size index (Figure 8). Disregarding the points with $Q_a^* > 1$ (obviously spoilt by experimental errors), it can be observed that most experimental points fall between the two curves, and are close to the upper curve. This is not surprising, as this upper curve is representative of high lighting conditions, as encountered in the surface layer. Also, the scatter of experimental points is expected because for a given size, $a_{cm}(440)$ can experience a large range of variation, because of variable pigment compositions and/or different photoacclimation states. In addition, several approximations have been introduced in these computations: (1) the theoretical values of $Q_a^*(440)$ are derived under some assumptions (sphericity and homogeneity of cells), (2) the biological noise likely affecting the $a_{miss}(440)$ variations with [Tchl *a*] is neglected, (3) each of the three phytoplanktonic classes is represented by a unique (central) size value, while their actual size range is rather large. Considering these various approximations, the agreement between experimental observations and theoretical predictions is encouraging, and suggests that (1) the values of $Q_a^*(440)$ and size index derived for each sample are compatible with realistic values of $a_{cm}(440)$, (2) the size index values derived from the concentrations of taxonomic pigments are consistent with the "bulk size" of populations (i.e., the size of the monodispersed population which would provide the same optical coefficients).

4. Conclusions

[36] In our former analysis of the natural variations of phytoplanktonic absorption [*Bricaud et al.*, 1995], we stated that the biological noise observed in the a_ϕ versus [Tchl *a*] relationships was "probably concealing specific and valuable information." The present analysis, based on an independent data set, confirms this statement. Significant deviations from the average $a_\phi(440)$ versus [Tchl *a*] relationships were observed, not only from one geographic zone to the other, but also seasonally within the same zone (e.g., within the Mediterranean Sea during the MINOS and PROSOPE cruises, respectively in May 1996 and September–October 1999).

[37] In many previous studies, the natural variability in the a_ϕ versus [Tchl *a*] relationships was attributed mostly to variations in the concentrations of accessory pigments (relatively to Tchl *a*). This statement has to be moderated, because even if the pigment composition of algal populations is known to vary largely for a given chlorophyll *a* content, the contributions of the various pigments may follow inverse trends (e.g., chl *b* and chl *c*, photosynthetic and nonphotosynthetic carotenoïds) and partially compensate one another, so that the actual impact on absorption is finally reduced. Our analysis showed that in most situations, the dominant cause of the deviations from the average a_ϕ versus [Tchl *a*] relationships is the size structure of algal populations, which may vary significantly for a given chlorophyll content. This was established using two independent approaches, one based on the package effect index (Q_a^*) at 440 nm, and the second one based on the estimate of a "size index" derived from the relative concentrations of some taxonomic pigments. The size index and $Q_a^*(440)$ show inverse variations and are quantitatively consistent with each other, which also suggests that the "size index" provides a realistic and usable information on the size structure of populations.

[38] The deviations from the average $a_\phi(440)$ versus [Tchl *a*] relationships, observed for some geographic areas, supports the existence of regional or seasonal relationships,

as already evidenced in previously published studies. This suggests that in some occasions, it might be appropriate to replace the global parameterizations by locally adapted relationships. HPLC measurements may be helpful to refine such parameterizations at a regional scale, to the extent that in a given area, they provide indirect information on the size structure of algal communities, and may help detecting ''atypical'' situations.

Appendix A: Estimation of the "Missing Term" in Algal Absorption

[39] We have observed, for many samples of our data set, that the experimental spectra for algal absorption ($a_\phi(\lambda)$) were higher than those reconstructed using HPLC measurements ($a_{sol}(\lambda)$; see text and equation (4)), while they should always be lower because of the package effect. Measurement uncertainties cannot be invoked as the cause of the observed differences, as they would introduce erratic noise on a_ϕ and a_{sol} values, instead of a systematic bias.

[40] Similar observations were made in previous studies [e.g., *Nelson et al.*, 1993]. These authors hypothesized that the differences could be due to ''missing pigments'' (carotenoids or phycobiliproteins, not measured by HPLC), or to other light-absorbing compounds (cytochromes, flavins, quinones..), extracted by methanol and thus included in the $a_\phi(\lambda)$ spectrum. *Bissett et al.* [1997], observing an offset in the $a_\phi(676)$ versus chl *a* relationship, suggested that cellular components could contribute to total absorption (and assumed this contribution was constant whatever the chl *a* concentration). The assumption that pigment-protein complexes have the same absorption spectra than those of the same pigments in solvent can also be questioned [see, e.g., *Johnsen et al.*, 1994]. To avoid this assumption, several attempts were made to derive the weight-specific absorption coefficients of the various pigments by deconvoluting the in vivo absorption spectra of phytoplankton into Gaussian bands [*Hoepffner and Sathyendranath*, 1991; *Lutz et al.*, 1996; *Stuart et al.*, 1998; *Wozniak et al.*, 1999; *Lohrenz et al.*, 2003]. It is striking to observe that in these studies, the amplitudes of the Gaussian bands are often significantly higher than the weight-specific absorption coefficients of the corresponding pigments in solvent, especially for chlorophylls *a*, *b* and *c* (see Table A1). Such differences can be explained either by weight-specific absorption coefficients higher in vivo than in solvent, or by the additional contribution of unidentified light-absorbing compounds.

[41] In the present study, we emit the hypothesis, as *Nelson et al.* [1993], that a term is missing when reconstructing the in vivo absorption spectrum of natural populations from pigment concentrations. The relative importance of this term appears to increase with decreasing pigment concentrations, as the discrepancies between measured and reconstructed absorption spectra are the most apparent for oligotrophic waters.

Table A1. In Vivo Weight-Specific Absorption Coefficients (a_{sol}*) of the Main Pigments at their Main Absorption Maximum, as Determined in Various Studies[a]

Pigment	Wavelength, nm	a_{sol}*	Method	Reference
chl *a*	440	0.0265	absorption in solvent	*Bidigare et al.* [1990]
chl *a*	440	0.0323	absorption in solvent	H. Claustre (unpublished data, 1997)
chl *a*	435	0.039[b]	Gaussian bands	*Hoepffner and Sathyendranath* [1991]
chl *a*	435	0.05–0.09	Gaussian bands	*Lutz et al.* [1996]
chl *a*	435	0.034–0.082	Gaussian bands	*Stuart et al.* [1998]
chl *a*	437	0.058	Gaussian bands	*Wozniak et al.* [1999]
chl *a*	435	0.039–0.047	Gaussian bands	*Lohrenz et al.* [2003]
chl *b*	470	0.0347	absorption in solvent	*Bidigare et al.* [1990]
chl *b*	466	0.0328	absorption in solvent	H. Claustre (unpublished data, 1997)
chl *b*	464	0.061[b]	Gaussian bands	*Hoepffner and Sathyendranath* [1991]
chl *b*	466	0.12–0.24	Gaussian bands	*Lutz et al.* [1996]
chl *b*	464	0.077–0.205	Gaussian bands	*Stuart et al.* [1998]
chl *b*	470	0.0514	Gaussian bands	*Wozniak et al.* [1999]
chl *b*	464	0.048–0.064	Gaussian bands	*Lohrenz et al.* [2003]
chl *c*	460	0.0708	absorption in solvent	*Bidigare et al.* [1990]
chl *c*	462	0.0760	absorption in solvent	H. Claustre (unpublished data, 1997)
chl *c*	461	0.051[b]	Gaussian bands	*Hoepffner and Sathyendranath* [1991]
chl *c*	461	0.04–0.16	Gaussian bands	*Lutz et al.* [1996]
chl *c*	461	0.094–0.298	Gaussian bands	*Stuart et al.* [1998]
chl *c*	460	0.072	Gaussian bands	*Wozniak et al.* [1999]
chl *c*	461	0.083–0.090	Gaussian bands	*Lohrenz et al.* [2003]
PSC	490	0.0368[c]	absorption in solvent	*Bidigare et al.* [1990]
PSC	490	0.0361[c]	absorption in solvent	H. Claustre (unpublished data, 1997)
PSC	490	0.038[b]	Gaussian bands	*Hoepffner and Sathyendranath* [1991]
PSC	490	0.03–0.05	Gaussian bands	*Lutz et al.* [1996]
PSC	490	0.0313	Gaussian bands	*Wozniak et al.* [1999]
PSC	490	0.034–0.038	Gaussian bands	*Lohrenz et al.* [2003]
PPC	462	0.0603[c]	absorption in solvent	*Bidigare et al.* [1990]
PPC	462	0.0545[c]	absorption in solvent	H. Claustre (unpublished data, 1997)
PPC	464	0.061[b]	Gaussian bands	*Hoepffner and Sathyendranath* [1991]
PPC	464	0.0253	Gaussian bands	*Wozniak et al.* [1999]

[a]Results based on the decomposition into gaussian bands are for natural populations, except those of *Hoepffner and Sathyendranath* [1991] which are for cultured phytoplankton.
[b]Determined on cultured phytoplankton.
[c]Average of several pigments.

[42] As these light-absorbing compounds are seemingly extracted by methanol but not identified by our HPLC measurements, we attempted to evidence this additional absorption by comparing the absorption spectra of methanol extracts and those reconstructed from HPLC measurements. Fourteen samples were collected in the NW Mediterranean (DYFAMED site, 28 miles off the French coast), at depths varying between 5 and 80 m. Samples (2.8 L) were filtered through Whatman GF/F filters, and filters were kept in liquid nitrogen for later analysis. In the laboratory, filters were thawed for a few minutes and put in 3 mL of methanol for at least one hour. Then the extracts were first spectrophotometrically analyzed, and then immediately analyzed by HPLC. Using the weight-specific absorption spectra of all individual pigments in methanol (as in Figure 1, but without spectral shifts), the absorption spectrum of pigments identified by HPLC could then be reconstructed for each sample, and compared to that of the extract. An incomplete extraction of pigments in methanol, if it occurs, does not influence the comparison since both analyses are performed on the same fraction of the extract.

[43] For all samples, absorption spectra of extracts were found to be systematically higher than reconstructed spectra. The difference spectra had carotenoïd-like spectral signatures (see example in Figure A1a). The excess absorption at 440 nm, $a_{miss}(440)$, covaries with [Tchl *a*] (Figure A1b), in contrast to the assumption made by *Bissett et al.* [1997]. A least square fit provides the following relationship:

$$a_{miss}(440) = 0.0525[\text{Tchl } a]^{0.855} \qquad \left(r^2 = 0.836, N = 14\right).$$

[44] This empirical relationship was used to estimate the term $a_{sol}(440)$ (see text and equations (4′) to (4‴)) and subsequently the package effect index at 440 nm, $Q_a^*(440)$ (equation (3)).

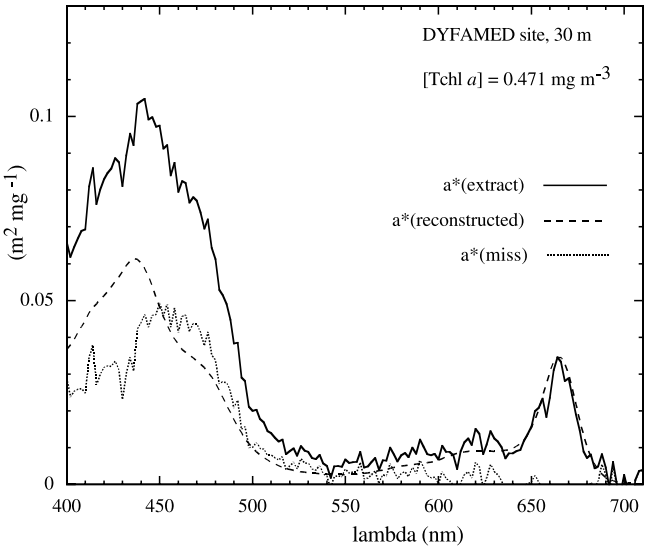

Figure A1a. Chl-specific absorption spectrum of a methanol extract (sample collected at 30 m at the Dyfamed site), as compared to the absorption spectrum reconstructed from the HPLC concentrations of individual pigments in this sample. The difference spectrum, a*(miss), is shown as a dotted line.

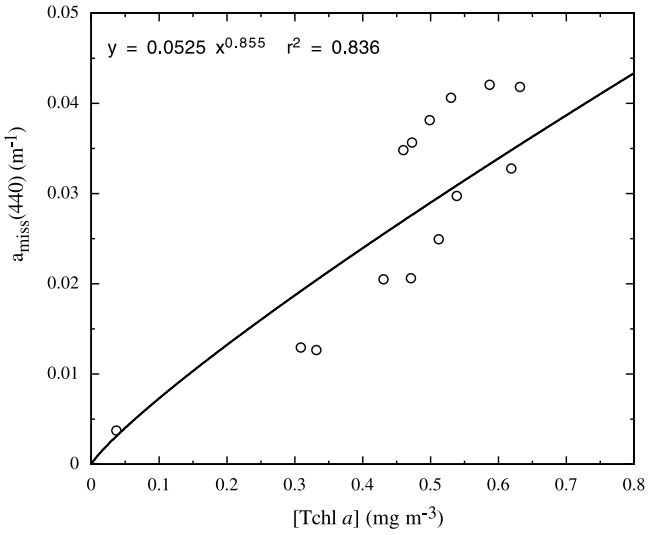

Figure A1b. Variations of the missing absorption term at 440 nm, $a_{miss}(440)$ (see Appendix A), as a function of the Tchl *a* concentration, for 14 samples collected between 0 and 80 m in the NW Mediterranean. The power function obtained by least square fit is shown as a solid line.

[45] **Acknowledgments.** This work is a contribution to several projects (EUMELI, EPOPE, FRONTAL, PROSOPE, POMME) funded by the PROOF (JGOFS-France) national program, and to the European project NAOC (EVG1-CT-2000-00034). The authors wish to thank the chief scientists and crews of the cruises during which the present data were collected, and the colleagues who participated to sample collection, HPLC measurements, or absorption measurements during some cruises: K. Allali, C. Cailliau, J. C. Marty, N. Sadoudi, D. Tailliez, F. Vidussi. They also thank A. Morel for suggestions on an earlier draft.

References

Allali, K., A. Bricaud, M. Babin, A. Morel, and P. Chang (1995), A new method for measuring spectral absorption coefficients of marine particles, *Limnol. Oceanogr.*, *40*, 1526–1532.

Allali, K., A. Bricaud, and H. Claustre (1997), Spatial variations in the chlorophyll-specific absorption coefficients of phytoplankton and photosynthetically active pigments in the equatorial Pacific, *J. Geophys. Res.*, *102*, 12,413–12,423.

Babin, M., D. Stramski, G. M. Ferrari, H. Claustre, A. Bricaud, G. Obolensky, and N. Hoepffner (2003), Variations in the light absorption coefficients of phytoplankton, nonalgal particles, and dissolved organic matter in coastal waters around Europe, *J. Geophys. Res.*, *108*(C7), 3211, doi:10.1029/2001JC000882.

Bidigare, R. R., M. E. Ondrusek, J. H. Morrow, and D. A. Kiefer (1990), In vivo absorption properties of algal pigments, *Proc. SPIE*, *1302*, 290–302.

Bissett, W. P., J. S. Patch, K. L. Carder, and Z. P. Lee (1997), Pigment packaging and Chl a-specific absorption in high-light oceanic waters, *Limnol. Oceanogr.*, *42*(5), 961–968.

Bricaud, A., and D. Stramski (1990), Spectral absorption coefficients of living phytoplankton and non-algal biogenous matter: A comparison between the Peru upwelling area and the Sargasso Sea, *Limnol. Oceanogr.*, *35*, 562–582.

Bricaud, A., M. Babin, A. Morel, and H. Claustre (1995), Variability in the chlorophyll-specific absorption coefficients of natural phytoplankton: Analysis and parameterization, *J. Geophys. Res.*, *100*, 13,321–13,332.

Bricaud, A., A. Morel, M. Babin, K. Allali, and H. Claustre (1998), Variations of light absorption by suspended particles with chlorophyll *a* concentration in oceanic (case 1) waters: Analysis and implications for bio-optical models, *J. Geophys. Res.*, *103*, 31,033–31,044.

Bricaud, A., H. Claustre, G. Obolensky, and M. Babin (2000), Light absorption by suspended particles and phytoplankton in case 2 waters, in

Ocean Optics XV Conference Papers [CD-ROM], Off. of Naval Res., Arlington, Va.

Carder, K. L., S. K. Hawes, K. A. Baker, R. C. Smith, R. G. Steward, and B. G. Mitchell (1991), Reflectance model for quantifying chlorophyll a in the presence of productivity degradation products, *J. Geophys. Res.*, *96*(C11), 20,599–20,611.

Chisholm, S. W. (1992), Phytoplankton size, in *Primary Productivity and Biogeochemical Cycles in the Sea*, edited by P. G. Falkowski and A. D. Woodhead, pp. 213–237, Plenum, New York.

Ciotti, A. M., J. J. Cullen, and M. R. Lewis (1999), A semi-analytical model of the influence of phytoplankton community structure on the relationship between light attenuation and ocean color, *J. Geophys. Res.*, *104*(C1), 1559–1578.

Ciotti, A. M., M. R. Lewis, and J. J. Cullen (2002), Assessment of the relationships between dominant cell size in natural phytoplankton communities and the spectral shape of the absorption coefficient, *Limnol. Oceanogr.*, *47*, 404–417.

Claustre, H., and J. C. Marty (1995), Specific phytoplankton biomasses and their relation to primary production in the tropical North Atlantic, *Deep Sea Res. Part I*, *42*, 1475–1493.

Cleveland, J. S. (1995), Regional models for phytoplankton absorption as a function of chlorophyll a concentration, *J. Geophys. Res.*, *100*, 13,333–13,344.

Goericke, R., and D. J. Repeta (1993), Chlorophylls *a* and *b* and divinyl-chlorophylls *a* and *b* in the open subtropical North Atlantic Ocean, *Mar. Ecol. Prog. Ser.*, *101*, 307–313.

Hoepffner, N., and S. Sathyendranath (1991), Effect of pigment composition on absorption properties of phytoplankton, *Mar. Ecol. Prog. Ser.*, *73*, 11–23.

Johnsen, G., N. B. Nelson, R. V. M. Jovine, and B. B. Prezelin (1994), Chromoprotein- and pigment-dependent modeling of spectral light absorption in two dinoflagellates, *Prorocentrum minimum* and *Heterocapsa pygmaea*, *Mar. Ecol. Prog. Ser.*, *114*, 245–258.

Kirk, J. T. O. (1975), A theoretical analysis of the contribution of algal cells to the attenuation of light within waters, II, Spherical cells, *New Phytol.*, *75*, 21–36.

Kishino, M., M. Takahashi, N. Okami, and S. Ichimura (1985), Estimation of the spectral absorption coefficients of phytoplankton in the sea, *Bull. Mar. Sci.*, *37*, 634–642.

Lee, Z., K. L. Carder, C. D. Mobley, R. G. Steward, and J. S. Patch (1998), Hyperspectral remote sensing for shallow waters, I. A semianalytical model, *Appl. Opt.*, *37*(27), 6329–6338.

Lohrenz, S. E., A. D. Weidemann, and M. Tuel (2003), Phytoplankton spectral absorption as influenced by community size structure and pigment composition, *J. Plankton Res.*, *25*(1), 35–61.

Lutz, V. A., S. Sathyendranath, and E. J. H. Head (1996), Absorption coefficient of phytoplankton: Regional variations in the North Atlantic, *Mar. Ecol. Prog. Ser.*, *135*, 197–213.

Malone, T. C. (1980), Algal size, in *The Physiological Ecology of Phytoplankton*, edited by I. Morris, pp. 433–463, Univ. of Calif., Berkeley, Calif.

Morel, A., and A. Bricaud (1981), Theoretical results concerning light absorption in a discrete medium, and application to specific absorption of phytoplankton, *Deep Sea Res.*, *28*, 1375–1393.

Morel, A., and S. Maritorena (2001), Bio-optical properties of oceanic waters: A reappraisal, *J. Geophys. Res.*, *106*, 7763–7780.

Nelson, N. B., B. B. Prezelin, and R. R. Bidigare (1993), Phytoplankton light absorption and the package effect in California coastal waters, *Mar. Ecol. Prog. Ser.*, *94*, 217–227.

Prieur, L., and S. Sathyendranath (1981), An optical classification of coastal and oceanic waters based on the specific spectral absorption curves of phytoplankton pigments, dissolved organic matter, and other particulate materials, *Limnol. Oceanogr.*, *26*, 671–689.

Sathyendranath, S., G. Cota, V. Stuart, H. Maass, and T. Platt (2001), Remote sensing of phytoplankton pigments: A comparison of empirical and theoretical approaches, *Int. J. Remote Sens.*, *22*(2–3), 249–273.

Stramski, D., A. Bricaud, and A. Morel (2001), Modeling the inherent optical properties of the ocean based on the detailed composition of the planktonic community, *Appl. Opt.*, *40*(18), 2929–2945.

Stuart, V., S. Sathyendranath, T. Platt, H. Maass, and B. D. Irwin (1998), Pigment and species composition of natural phytoplankton populations: Effect on the absorption spectra, *J. Plankton Res.*, *20*(2), 187–217.

Van de Hulst, H. C. (1957), *Light Scattering by Small Particles*, John Wiley, Hoboken, N. J.

Vidussi, F., H. Claustre, J. Bustillos-Guzman, C. Cailliau, and J. C. Marty (1996), Rapid HPLC method for determination of phytoplankton chemotaxinomic pigments: Separation of chlorophyll *a* from divinyl-chlorophyll *a*, and zeaxanthin from lutein, *J. Plankton Res.*, *18*, 2377–2382.

Vidussi, F., H. Claustre, B. B. Manca, A. Luchetta, and J. C. Marty (2001), Phytoplankton pigment distribution in relation to upper thermocline circulation in the eastern Mediterranean Sea during winter, *J. Geophys. Res.*, *106*(C9), 19,939–19,956.

Wozniak, B., J. Dera, D. Ficek, R. Machrowski, S. Kaczmarek, M. Ostrowska, and O. I. Koblentz-Mischke (1999), Modelling the influence of acclimation on the absorption properties of marine phytoplankton, *Oceanologia*, *41*(2), 187–210.

Yentsch, C. S., and D. A. Phinney (1989), A bridge between ocean optics and microbial ecology, *Limnol. Oceanogr.*, *34*, 1694–1705.

A. Bricaud, H. Claustre, and J. Ras, Laboratoire d'Océanographie de Villefranche, CNRS and Université Pierre et Marie Curie, BP 08, F-06238 Villefranche-sur-Mer, France. (annick@obs-vlfr.fr)

K. Oubelkheir, Environmental Remote Sensing Group, CSIRO Land and Water, GPO Box 1666, Canberra, ACT 2601, Australia.